Research into a Single-Aperture Light Field Camera System to Obtain Passive Ground-based 3D Imagery of LEO Objects

Kenneth P. Bechis
Northrop Grumman Information Systems
Andover, MA
Ann M. Pitruzzello
Northrop Grumman Information Systems
Morrisville, NC

ABSTRACT

This presentation describes our ongoing research for using a ground-based light field camera to obtain passive, single-aperture 3D imagery of low earth orbit (LEO) objects. Light field cameras are an emerging and rapidly evolving technology for passive 3D imaging with a single optical sensor. The cameras use an array of lenslets placed in front of the camera focal plane, which provides angle of arrival information for light rays originating from across the target, allowing range to target and a 3D image to be obtained from a single image using monocular optics. The technology, which has been commercially available for less than four years, has the potential to replace dual-sensor systems such as stereo cameras, dual radar-optical systems, and optical-LIDAR fused systems, thus reducing size, weight, cost, and complexity. We have developed a prototype system for passive ranging and 3D imaging using a commercial light field camera and custom light field image processing algorithms. Our light field camera system has already demonstrated its utility for nearby ground-target surveillance and threat detection applications, and this paper presents results of our research thus far into applying the technology to multi-kilometer long-range 3D imaging, with the ultimate objective being the passive 3D imaging of LEO objects.

1. INTRODUCTION

There are numerous research papers and review articles describing the theory, design principles, and image processing techniques for light field cameras (e.g., references [1], [2], [3], and [4], *inter alia*). This paper will provide only a brief overview of the camera concept of operation, and will instead describe results from experiments designed to identify and evaluate those light field camera design parameters most relevant to developing its capability to obtain passive, single-aperture, ground-based 3D imagery of low earth orbit (LEO) objects.

The optical components available to us for these experiments – a Meade 14" Advanced Coma Free LX600 catadioptric telescope and a Raytrix R5 light field camera – we knew *a priori* were inadequate to obtain 3D imagery of LEO objects. However, we incorporated them into long-range (up to 2 km) horizontal line-of-sight imaging experiments to explore camera design sensitivities, achievable target 3D imagery quality, and other factors scalable to what would be required for LEO object 3D imaging.

The observations were conducted in the spring of 2014, in the vicinity of the Northrop Grumman Corporation Colorado Springs facility, adjacent to the Colorado Springs Airport. All the measurements were made within one to two hours of sunrise, to minimize thermals and wind turbulence that would later develop and degrade the seeing along a horizontal line of sight.

2. BACKGROUND

Light field cameras are an emerging technology for single-camera, passive 3D imaging. The first commercial camera was available from Raytrix in 2010. They are currently manufactured by Raytrix and Lytro (which focuses more on the consumer-grade market). For scientific/technical applications, the light field camera has been used predominantly for close-range laboratory inspection, production quality control, biological research, and 3D microscopy [1], [5]. However, to our knowledge this technology has not previously been used for long-range 3D imaging. This is because an essential requirement for light field camera operation is that the target must be in the near-field (Fraunhofer distance) of the collecting optics. This is defined as $2D^2/\lambda$, where D is the diameter of the collecting optics aperture. For λ in the center of the visible light band (0.565×10^{-6} m), the near-field of a 1-m telescope extends out to about 3,500 km, and the near-field of the AEOS telescope extends over 46,000 km.

A light field camera uses a microlens array, positioned just in front of the CCD sensor focal plane, to capture angle-of-arrival information for light rays originating from across the target. Consequently, the larger the image of the target appears on the focal plane, the greater the area that can be sampled by the lenslet array for light ray angle-of-arrival information, and hence the better the quality and precision of the resulting 3D imagery. Fig. 1 provides a schematic of this process, and a depiction of the "honeycomb" pattern seen in raw light field images produced by the thousands of microlenses in the lenslet array. In the enlargement, the subject's face occurs in each of the subimages, but viewed at slightly different angles, resulting from the physical geometry of the microlens array. Analysis of the different angles of arrival of light from the target provide the means to derive the 3D characteristics of the surface being imaged, as well as information that can contribute to target range determination.

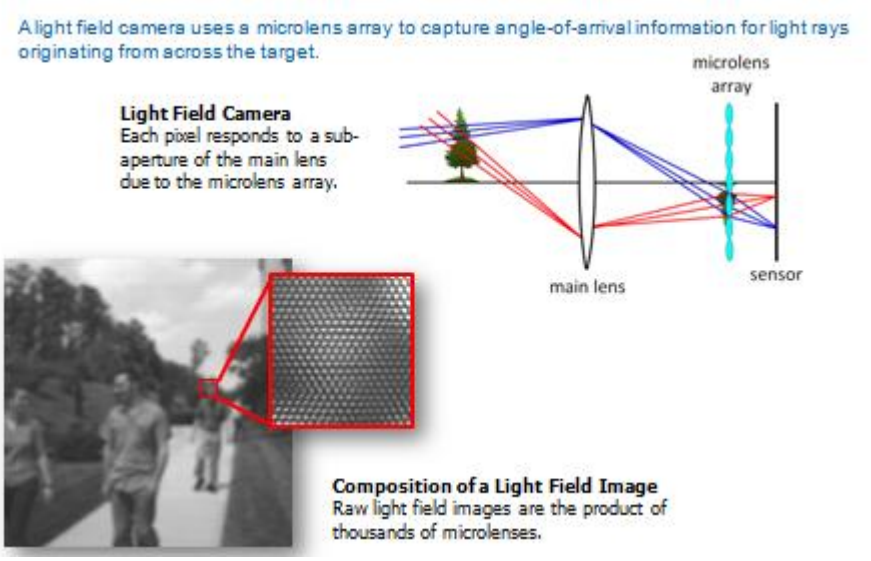

Fig. 1. How the light field camera technology works

3. EXPERIMENT SENSOR HARDWARE, SOFTWARE, AND TARGETS

For our initial proof of concept experiments, we integrated our existing light field camera with a 14" Meade LX600 advanced coma-free telescope to image various surrogate ground targets at up to several kilometers range. Our experiments with the 14" telescope have assessed factors and requirements that are traceable and scalable to a larger-aperture system that would have the near-field distance needed to obtain 3D images of LEO objects. A major objective was to examine the expected performance shortfalls of our existing camera, including the sensitivity of

depth determination accuracies to changes in component f/#'s and optical system magnification. These observations would help determine what optical design characteristics in the overall system (camera and telescope) would need to be optimized to best accomplish long-range 3D imaging, and the sensitivity of the 3D image quality to deviations from optimal optical designs.

Fig. 2 and 3 depicts the experimental hardware set up outside the Northrop Grumman facility in Colorado Springs, CO. Fig. 4 shows the Raytrix R5 light field camera alone; Fig. 5 provides a closer view of the camera mounted at the focus of the 14" Meade LX600 telescope.

Fig. 2. Meade 14" LX600 telescope with Raytrix R5 light field camera at Colorado Springs, CO, test range

Fig. 3. Meade 14" LX600 telescope with Raytrix R5 light field camera pointed at target location

Fig. 4. Raytrix R5 light field camera (f/2.4 lenslet array)

Fig. 5. Raytrix R5 light field camera installed with f/6.3 focal reducer on 14" Meade LX600 telescope

Experiment instrumentation:

- Telescope: 14" Meade LX600 advanced coma free catadioptric telescope
  - f/8 (2845 mm focal length) at prime focus
  - Effective f/5 with an f/6.3 focal reducer
  - Effective f/24 with a 15mm f.l. eyepiece
  - Effective f/15 with 15mm f.l. eyepiece and f/6.3 focal reducer

- Light field camera
    - Raytrix R5 C2GigE camera
    - Frame rate: up to 30 frames per second
    - Depth resolution: up to 100 discrete layers
    - Microlens f/#: f/2.4
- Image acquisition and processing
    - Windows computer with nVidia GPU; light field images acquired to disk
    - User can configure for automated camera triggering
    - Raytrix software, and Northrop Grumman custom software developed for processing long-range 3D images
        - Image refocusing
        - Depth map/range finding
        - Optional processing modules (change detection; 3D reconstruction)

Fig. 6 describes the software processing flow, ending in several optional processing modules (including one which is appropriate for long-range terrestrial applications such as 3D detection/identification of faces).

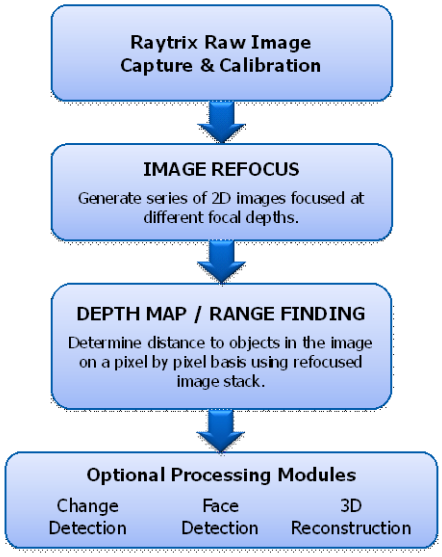

Fig. 6. Long-range 3D imagery data processing flow, incorporating custom Northrop Grumman software

The first step in the image acquisition process involves focusing the telescope on the target. Focusing on the closest portion of the target helps maximize the number of focus planes that the light field camera will be able to apply against the target. For the f/2.4 light field camera used here, the number of focus planes, corresponding to depth bins, can be up to 100 in an optimized telescope/camera system; this is chiefly determined by the number of lenslets in the array in front of the camera focal plane. However, the number and resolution of the useable depth bins will decrease as mismatches between the f/#'s of the lenslet array and the telescope increase. We observed this effect in our experiments, because of the mismatch between the f/#'s of the telescope and the light field camera. For 3D imaging of LEO objects, the light field camera and the tracking telescope f/#'s should be matched, and the telescope will presumably know the target range at all times and be able to adjust its focus automatically.

The importance of matching the f/#'s of the collection optics and the light field camera lenslet array is depicted in Figs. 7 and 8. Deviating from the goal of matched f/#'s (i.e., having $F = F_L$ as shown in Fig. 7) will progressively reduce the illumination of each lenslet, with a consequent reduction in achievable angular and depth resolution.

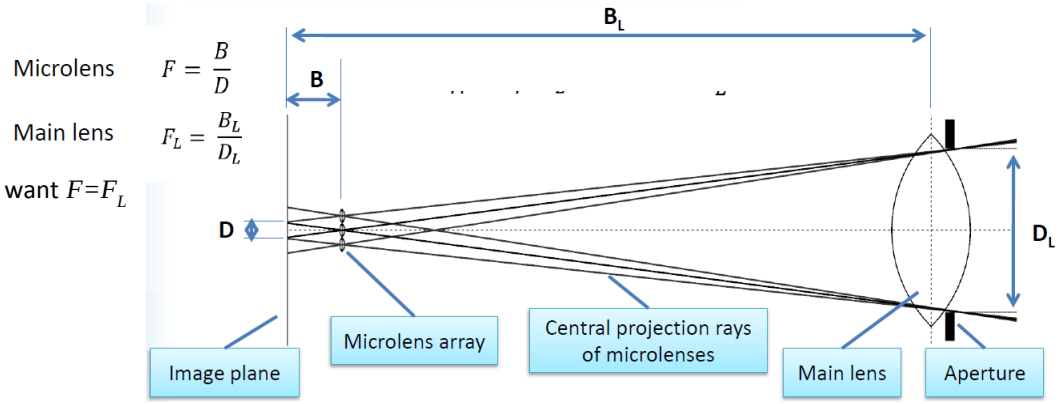

Fig. 7. Light field camera f/# matching [5]; optimum goal: F = F_L

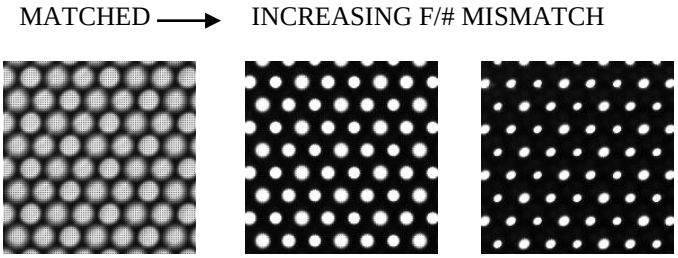

MAIN APERTURE:	f/2.4	f/8	f/24
LENSLET ARRAY:	f/2.4	f/2.4	f/2.4

Fig. 8. Calibration images of lenslet (i.e., microlens) pattern imaged directly on sensor array; f/# mismatch results in net lost angular and depth resolution in reconstructed 3D image

After the raw image data has been captured by the Raytrix camera, it is transmitted to the camera control/data acquisition/processing computer containing an nVidia graphics processing unit (GPU) for storage and subsequent analyses. The system has a frame rate of 30 Hz, and the software control interface allows for automated camera triggering and light field image acquisition to disk. As shown in Fig. 6, a combination of Raytrix and custom Northrop Grumman software then performs the following steps: (1) image refocusing, (2) change detection, (3) range finding, and (4) 3D reconstruction. In Step (1), a series of 2D images are generated from each light field image; as described above, for an optically optimized/matched system the 2D images can be refocused at up to 100 different depths. Currently steps (1) and (2) are automated, while steps (3) and (4) require some user interaction.

3D imaging experiments were performed against three different targets, during two collection periods in Spring 2014. A large SUV (Fig. 9) positioned to have distinctive depth structure, a scale model of a notional satellite called Trinidad (Fig. 10), and a 4.5-m diameter ground station antenna (Fig. 11).

4. EXPERIMENTAL RESULTS

Fig. 12 shows, on the left, the light field camera image of the SUV and, on the right, a depth map. Fig. 13 shows the depth map overlaid on the image. The estimated range resolution is approximately 0.6 – 0.8 m; the imagery demonstrates the ability to resolve multiple depth layers within the target, as well as individual 3D features such as the open front passenger door and window, and the open rear passenger door with closed window. The apparent

low-quality of the data product, despite demonstrating the capability to collect long-distance 3D imagery, is directly attributable to the significant mismatch between the f/# of the telescope (f/8) and the f/# of the light field camera lenslet array (f/2.4) at the telescope's prime focus. The f/# of the telescope could not be reduced for these measurements. Experimenting with higher effective telescope f/#'s (by inserting eyepieces in the optical train) significantly worsened the depth measurement resolution.

Fig. 9. Target 1: Nissan Xterra SUV, with front passenger door and window open; Range = 1.38 km

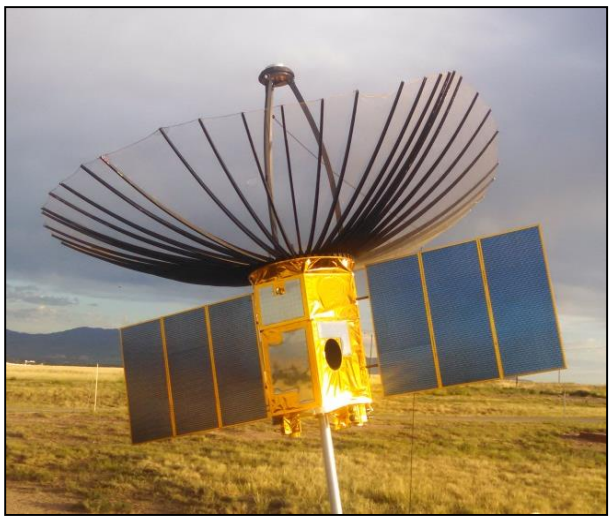

Fig. 10. Target 2: Scale model of notional Trinidad satellite; Range = 1.38 km

Fig 11: Target 3: 4.5-m ground station antenna; Range = 0.7 km

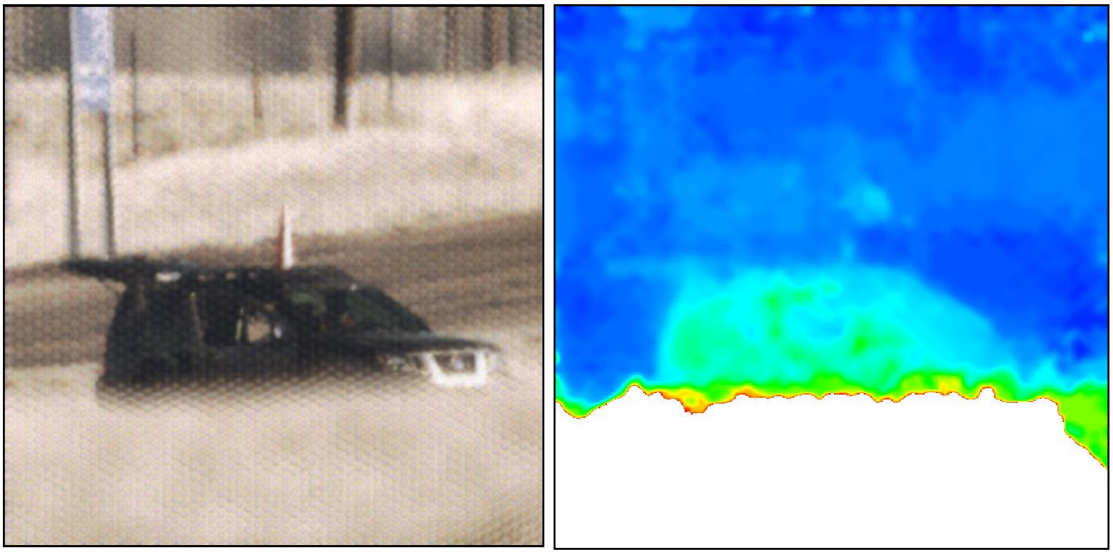

Fig. 12. Light field camera image (left) digitally refocused at a single focus plane, and depth map (right)

Fig. 14 shows the results of imaging the Trinidad satellite model. The diameter of the opened mesh antenna and the width of the solar panel array were both approximately 2 meters, considerably smaller than the SUV. Additionally, depth information was not able to be gathered from most of the semi-transparent mesh surface. With a focal reducer, we reduced the f/# of the telescope to f/5, bringing it closer to the f/2.4 of the lenslet array. However, that also reduced the image size to an unacceptably small scale. Increasing the telescope/s f/# to f/15 significantly magnified the size of the satellite model's image; however it exacerbated the honeycomb appearance, by increasing the f/# mismatch between telescope and lenslet array and reduced the achievable depth resolution by reducing the diversity of the light rays' angles of arrival, and reducing the number of illuminated sensor pixels. Nevertheless, even under these distinctly non-optimal conditions, the significantly larger image size of target allowed some depth information to be derived (e.g., the forward tilt of the solar panels, the slightly more distant receiver box at the apex of the prime focus support rods).

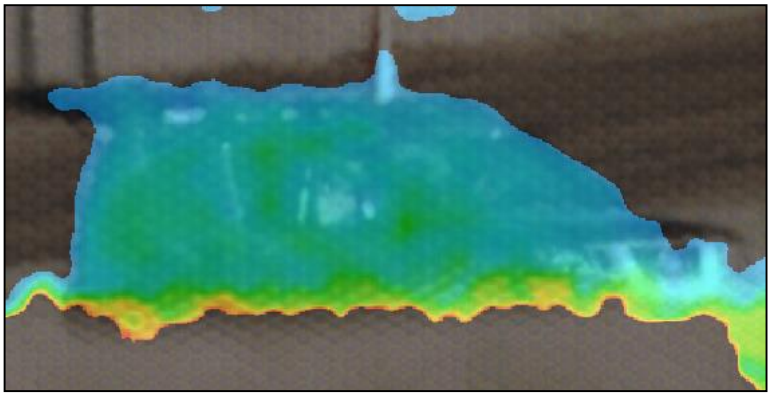

Fig.13. Depth map overlaid on light field camera image, depicting 0.6 – 0.8 m estimated depth resolution.

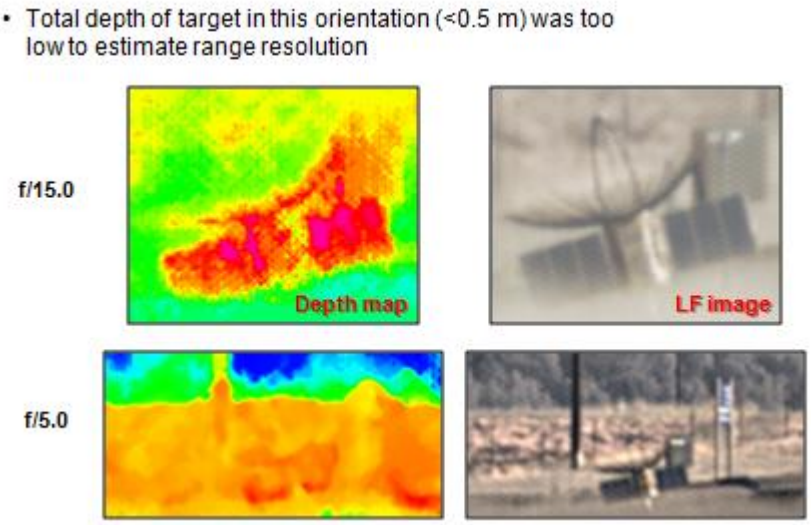

Fig. 14. Results of satellite model imaging, with telescope at f/15 (top) and f/5 (bottom)

Fig. 15 shows the results of imaging the 4.5-m ground station antenna. Note that in the basic light field camera image (LF image) on the left, the tilt and/or pointing orientation of the antenna cannot be discerned. The antenna is in fact pointing up and to the left. That tilts the back upper left quadrant of the antenna toward and closer to the light field camera, with the closest areas indicated in red (i.e., at ~0 meters relative depth) and the most distant areas (toward the lower right, diametrically opposite the red areas) indicated in blue. The depth resolution in this image, through still not optimum, is better than that depicted in Fig. 13 because the f/#'s of the telescope and lenslet array are a closer match (here, f/5 vs. f/2.4, as opposed to f/8 vs. f/2.4 in Fig. 13), and the target image more fully filled the lenslet array/focal plane, hence maximizing the diversity of light ray angle-of-arrival measurements that the lenslet array/focal plane could measure.

5. CONCLUSIONS AND RECOMMENDATIONS

Our experiments confirm that long-distance passive 3D imaging using commercially available equipment (a light field camera and appropriate front-end optics/telescope) is achievable. The highest depth resolutions can be achieved by adjusting the effective f/# of the front-end optics a) to match as closely as possible – without going below -- the fixed f/# of the camera's lenslet array, and b) to maximize target image size on the camera focal plane. Requirement b) obviously requires that some *a priori* knowledge/estimate of the target apparent angular size

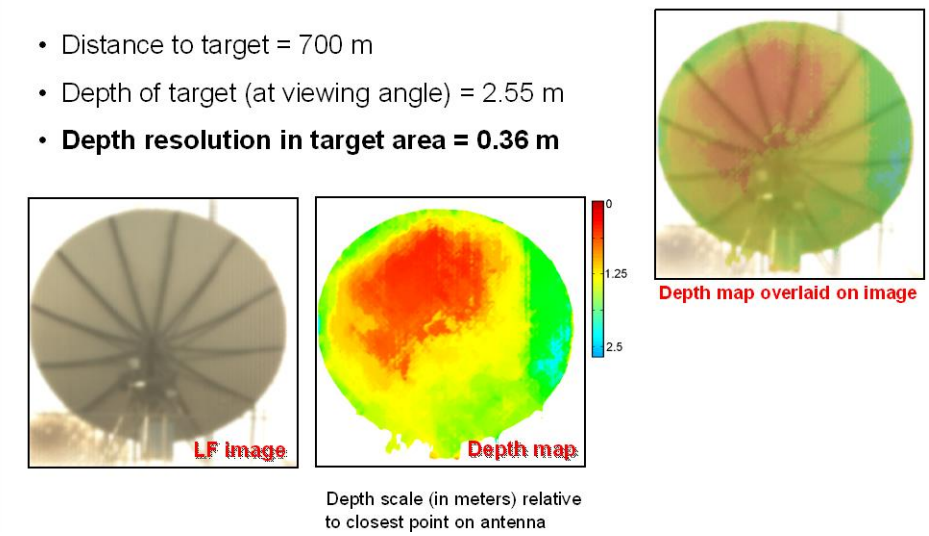

Fig. 15. Results of 4.5m ground station antenna imaging, with telescope at f/5, showing depth resolution of 0.36m

(derivable in part from knowledge of target physical size and range), is needed before the collection. This knowledge may in turn drive the specification of the f/# of the lenslet array/light field camera that would best facilitate matching the f/#'s of the front-end optics and the lenslets. Imaging scenarios where target range and hence apparent angular size are changing (e.g., when observing LEO satellites) will need to be addressed through real-time adjustments in the magnification provided by the front-end optics without compromising Requirement a) above, as no modification in the f/# of the light field camera's lenslet array can be done during imaging.

In applying the light field camera technology to the 3D imaging of LEO satellites, several additional considerations must be taken into account. The telescope must be able to track LEO satellites, and have sufficient aperture that the ranges of satellites of interest fall well within its near field (Fraunhofer distance). Also, an adaptive optics system for atmospheric turbulence/wavefront sensing and cleanup appears advisable, though there is a possibility, as yet unevaluated, that the light field camera, with its lenslet array virtually identical in form and function to those found in Shack-Hartmann wavefront sensors, may itself be able sense and correct wavefront errors in post-detection processing.

6. ACKNOWLEDGEMENTS

The authors acknowledge the invaluable support during the data collection campaigns provided to us by Mr. Steve Wilcox. We also acknowledge additional engineering support provided by Mr. James Spence, and helpful technical discussions with Mr. Kevin Giammo and Mr. Jim Przybysz. All the acknowledged personnel are with Northrop Grumman Information Systems in Colorado Springs, CO.

7. REFERENCES

1. Ng, R., *Digital Light Field Photography*, Ph.D. Dissertation, Stanford University Computer Science Dept., 2006.
2. Adelson, E.H., and Wang, J.Y.A., Single lens stereo with a plenoptic camera, IEEE *Transactions on Pattern Analysis and Machine Intelligence*, Vol. 14, 2 (Feb), 99-106, 1992.
3. Isaksen, A. et al, Dynamically reparameterized light fields, SIGGRAPH, 297-306, 2000.
4. Deans, S.R., *The Radon Transform and Some of Its Applications*, Wiley-Interscience, New York, 1983.
5. Raytrix company online brochure, www.raytrix.de/tl_files/downloads/Raytrix_Slides.pdf, 23, 2012.